

CHAPTER IV
IMPROVEMENT OF DUAL-LEACHED POLYCAPROLACTONE POROUS
SCAFFOLDS BY INCORPORATED WITH HYDROXYAPATITE FOR
BONE TISSUE REGENERATION

4.1 Abstract

Polycaprolactone(PCL)/hydroxyapatite(HA) composite scaffolds were prepared by combining solvent casting and salt particulate leaching with polymer leaching technique. The dual-leached scaffold was improved hydrophilicity by alkaline treatment (NaOH treatment). Well defined and interconnected pores were detected by scanning electron microscope (SEM) analysis. The water absorption capacity of NaOH treated PCL/HA dual-leached scaffold were most increased which confirmed the hydrophilicity of the scaffold was improved by NaOH treatment. The compressive modulus of the PCL/HA dual-leached scaffolds was greatly increased by the addition of HA particles. An indirect cytotoxicity evaluation of all PCL dual-leached scaffolds with mouse fibroblastic cells (L929) and mouse calvaria-derived pre-osteoblastic cell (MC3T3-E1) indicated PCL dual-leached scaffolds were posed as nontoxic to cells. The ability to support mouse calvaria-derived pre-osteoblastic cell (MC3T3-E1) attachment, proliferation, differentiation, and mineralization were also evaluated. Despite the viability of cells on PCL/HA dual-leached scaffold was lower than that on tissue-culture polystyrene plate (TCPS) and the others at early time points, both PCL and NaOH treated PCL/HA dual-leached scaffolds supported the attachment of MC3T3-E1 at significantly higher levels to TCPS. During the proliferation period (day 1-3), all PCL dual-leached scaffolds were able to support the proliferation of MC3T3-E1 at higher levels to that cells on TCPS, with the cells grown on NaOH treated PCL/HA dual-leached scaffold showing the greatest proliferation rate. For mineralization, cells cultured on surfaces of NaOH treated PCL/HA dual-leached scaffold showed the highest mineral deposition.

(Key-words: Scaffold, PCL, Solvent casting/Particulate leaching method, dual- leached scaffold, Hydroxyapatite)

4.2 Introduction

Tissue engineering originates in reconstructive surgery, a field that involves the replacement of organs to repair the function of damaged tissue.¹ Many research groups are involved in tissue engineering, and tissue engineering constructs have significantly improved in recent years.² One of the major topics of investigation in the field is scaffold fabrication. Scaffolds represent the space available for tissue development; they act as physical supports for cell growth before the cells are transplanted back to the host tissue. To be compatible with the structure of the tissue, scaffolds should have a specific three-dimensional shape, high porosity, a fully interconnected geometry, a large surface area, and structural strength. Scaffold porosity and interconnected geometry are fundamental characteristics necessary for promoting cell growth, blood vessel invasion, and effective metabolic nutrient/waste transport. Additionally, the highly specific surface area and high porosity of scaffolds allow cell attachment to occur and promote cell growth and migration and the effective transportation of fluids and nutrients. The mechanical properties of the scaffold should allow the structure to maintain its shape during tissue regeneration and enable the transfer of stress and load bearing.¹⁻⁴

Aliphatic polyesters (e.g., polycaprolactone (PCL)⁵⁻¹¹, poly(L-lactide) (PLLA)¹²⁻¹⁵, and poly(lactide-co-glycolide) (PLGA)¹⁶⁻¹⁷) are attractive materials for the construction of scaffolds to be used in tissue engineering, as they are FDA-approved biodegradable polymers with remarkable toughness and good biocompatibility.^{7,18-19} In particular, PCL is a semi-crystalline aliphatic polymer with sustained biodegradability and good biocompatibility; in addition, it is expected to be bioresorbable.^{6,10,20}

Of the numerous bioceramics available, bioactive glass, silica, tricalcium phosphate, biphasic calcium phosphate, and hydroxyapatite (HA) have been widely investigated for use in bone tissue engineering.¹¹ Hydroxyapatite (HA) is one of the most extensively investigated materials because its composition and structure resemble those of the minerals that form natural bone. HA ($\text{Ca}_{10}(\text{OH})_2(\text{PO}_4)_6$) has been demonstrated to have good biocompatibility, good biological properties (osteoconductivity and osteoinductivity), and sufficient mechanical stability.^{5,10,21-27}

However, HA is difficult to mold into complex shapes and unsuitable for load-bearing applications because of its stiffness and brittleness.^{26,28}

Composite materials have been widely studied and used for the development of scaffolds for bone tissue engineering. Composites, or nano-composite materials made with a polymeric matrix and ceramic reinforcers such as hydroxyapatite (HA), tricalcium phosphate (TCP), silica or bioactive glass, have been proposed for the fabrication of porous materials with adequate mechanical properties for bone tissue engineering.^{11,29} The main disadvantage of polymeric scaffolds is their low mechanical strength; the main disadvantage of ceramic scaffolds is their inherent brittleness.²¹ One possible way to overcome these problems is to fabricate composite scaffolds that combine the toughness of the polymer component with the strength and stiffness of the ceramic component; such a composite scaffold would have superior mechanical properties.^{9,11,25,30} Wei et al. showed that introducing HA into HA/polymer composite scaffolds greatly increased the mechanical properties of the scaffold and improved its protein adsorption capacity.²¹ Many studies have confirmed that the incorporation of ceramics into polymer scaffolds can improve the mechanical properties and protein adsorption of the composite scaffolds. Moreover, the combination of polymers with bioceramics has also improved the osteoconducting properties of scaffolds.^{10,13,15}

Several techniques have been developed to fabricate scaffolds. These include solvent casting combined with particulate leaching, freeze drying, electrospinning, phase separation, melt molding, and combinations of these techniques. Solvent casting combined with particulate leaching is a technique that results in highly porous structures.²⁰ The main advantage of this technique is that it facilitates fabrication by eliminating the need for specialized equipment.²⁸ The polymer is dissolved into a suitable solvent and mixed with a porogen; then, the solution is cast into a 3-D mold. The porogen can consist of gelatin or paraffin spheres, saccharose crystals, or an inorganic salt such as sodium chloride (NaCl). After the solvent evaporates, the water-soluble porogen is leached away by using water to form the pores of the scaffold.^{1,3,31}

In our previous work³², a PCL scaffold with highly interconnected networks was fabricated with a technique involving our modified solvent casting, particulate

leaching, and polymer leaching, with a solution of sodium chloride and polyethylene glycol (PEG) used as a porogen. Although this solution increased the porosity of the scaffold and produced an interconnected network to facilitate bone ingrowth, the mechanical properties of the scaffold were inferior. A scaffold should not only be highly porous and have good pore connectivity to ensure sufficient nutrient and waste transport but also have suitable mechanical properties that are comparable to those of the living tissue at the site of implantation.³³ The aim of the present study was therefore to improve the mechanical properties of the dual-leached PCL scaffold by adding hydroxyapatite. Because PCL has a hydrophobic nature, an alkaline (NaOH) treatment of the PCL/HA dual-leached scaffold is required to improve the water retention capacity of the scaffold. The morphologic, physical, and mechanical properties of the PCL and PCL/HA dual-leached scaffold were investigated. Finally, the indirect cytotoxicity of the scaffold to L929 cells and MC3T3-E1 cells was investigated; additionally, the attachment, proliferation, and differentiation of MC3T3-E1 cells were evaluated to determine the potential of scaffolds to be used in bone-tissue engineering.

4.3 Experimental

4.3.1 Materials

Polycaprolactone (PCL; MW = 80,000 gmol⁻¹) and calcium hydroxide (Ca(OH)₂) were purchased from Sigma-Aldrich, USA. Phosphoric acid (H₃PO₄) and chloroform were purchased from Labscan (Asia), Thailand. Sodium hydroxide (NaOH) was purchased from Carlo Erba, Italy. Polyethylene glycol (PEG; MW = 1,000 gmol⁻¹) was purchased from Merck, Germany. Sodium chloride (Ajax Finechem, Australia) was used as a porogen. All other chemicals were of analytical reagent grade and used without further purification.

4.3.2 Preparation of PCL, PCL/HA and NaOH Treated PCL/HA Scaffolds

Hydroxyapatite powder was synthesized according to the procedure proposed by Lee et al.³⁴ Both neat PCL and PCL/HA dual-leached scaffolds were fabricated with a technique involving solvent casting, polymer leaching, and salt

particulate leaching. Equal masses of PCL and PEG were first dissolved in chloroform at a concentration of 28% w/v to obtain a blended solution of the polymers. Next, HA powder (0-50% w/w of PCL) was added to the solution. NaCl particles were sieved to obtain particles with diameters in the range of 400-500 μm and added to the PCL and PCL/HA solutions (PCL: NaCl ratio=1:30). The mixture was then packed into Petri dishes, and a cylindrical mold with a diameter of 1.2 mm and a thickness of 0.8 mm was formed. The molds were placed in a fume hood overnight for solvent evaporation. Subsequently, the materials were immersed in deionized (DI) water for 48 hours; the water was changed every 8 hours to allow the PEG and salt particles to leach out. Scaffolds were air-dried for 24 hour and vacuum-dried overnight. To improve hydrophilicity, scaffolds were immersed in 1 M NaOH aqueous solution at 37 °C for 1 hour. The NaOH-treated scaffolds were rinsed with DI water and dried *in vacuo* for 48 hours.³⁵⁻³⁶ For purposes of sterilization, the scaffolds were placed in 70% v/v ethanol for 30 min and washed with sterile DI water.

4.3.3 Characterization of HA

For the morphological study, hydroxyapatite was mounted on brass stubs, coated with gold using a JEOL JFC-1100 sputtering device, and observed with a JEOL JSM-5200 scanning electron microscope (SEM).

The microstructural and morphological features of HA powders were analyzed in a JEM-2100 with an operating voltage of 200 kV. Samples for TEM were prepared by air-drying a drop of a sonicated ethanol suspension of particles on a carbon-coated copper grid.

The Ca/P ratio of the hydroxyapatite was studied by X-ray microanalysis using the method of Energy dispersive X-ray spectroscopy (EDS). EDS is an analytical technique that was used to determine the elemental composition of the HA.

The phase compositions, crystal shape, and crystal size of HA powders were characterized by X-ray diffraction (XRD) with a copper target. Data were collected over the scanning range (2θ) from 5 ° to 70° with a 0.02° scanning

step. The average crystallite size of the prepared hydroxyapatite samples was determined with the Scherrer equation.

$$D = \frac{K \cdot \lambda}{\beta \cdot \cos \theta}$$

In this equation, D is the average crystallite size (Å), K denotes the shape factor (K=0.9), λ is the X-ray wavelength (for CuK α , $\lambda=1.5418$ Å), β represents the peak at half width (in rad), and θ is the Bragg angle of the peak (002 reflection of hydroxyapatite at $2\theta=26^\circ$).

4.3.4 Characterization of PCL, PCL/HA and NaOH Treated PCL/HA Scaffolds

The pore morphology, pore size, and distribution and interconnectivity of pores were observed with a JEOL JSM-5200 scanning electron microscope (SEM). One cylindrical scaffold was randomly selected from each group, cut in the middle with a razor blade, and mounted onto an SEM stub. Cross sections of the scaffolds were coated with a thin film of gold using a JEOL JFC-1100E sputtering device 5 min prior to observation by SEM.

Porosity and pore volume of the scaffolds were measured gravimetrically and calculated according to the following equations:

$$Porosity(\%) = \left(1 - \frac{\rho_{\text{scaffold}}}{\rho_{\text{polymer}}}\right) \times 100$$

$$Pore\ volume(\%) = \left(\frac{1}{\rho_{\text{scaffold}}} - \frac{1}{\rho_{\text{polymer}}}\right) \times 100$$

Here, ρ_{polymer} is the density of the polymer used to fabricate the scaffold, and ρ_{scaffold} is the apparent density of the scaffold as measured by a Sartorius YDK01 density measurement kit. The ρ_{PCL} value was assumed to be 1.145 g cm^{-3} . The porosity and the pore volume of 10 specimens were measured, and an average value for each property was calculated. In contrast, pore size was directly measured from the SEM images with a SemAfore Digital slow scan image recording system, software version 5.0. At least 30 pores were measured, and average values were calculated for all of the scaffolds investigated.

The scaffold specimens were cut from the moldings that had been cast in the Petri dishes. Thus, the specimens were cylindrical with a diameter of 15 mm and a height of 3 mm. The specimens were dried and weighed, and each specimen was immersed in 10 mL of 10 mM phosphate buffered saline solution (PBS; pH 7.4) at room temperature. At selected time points, the specimens were removed, carefully placed on the glass for 5 sec to remove excessive water, and immediately weighed. The amount of water retained in each specimen was determined according to the following equation:

$$\text{Water absorption}(\%) = \frac{(W_w - W_d)}{W_w} \times 100$$

where W_d and W_w are the weights of the specimen before and after submersion in the medium, respectively. The experiment was carried out in triplicate, and measurements were taken at different times over a period of 3 days.

A Mettler Toledo thermogravimetric analyzer/differential scanning calorimeter (TGA/DSC 1) was used to determine the actual amount of HA within the PCL/HA dual-leached scaffolds. Each specimen was heated from 25 °C to 900 °C at a rate of 20 °C/min.

The compressive modulus of each scaffold was determined with a universal testing machine (Lloyd LRX, UK) using a 500 N loaded cell in a dry state at room temperature. The scaffolds were vertically compressed at a crosshead speed of 3 mm/min. The load was applied until the scaffolds were compressed to approximately 70% of their original thickness. The initial compressive modulus was determined as the slope of the linear portion of the stress-strain curve at a compressive strain of 20%.

To obtain information on pore interconnectivity, the flow resistance of the constructs was evaluated by sealing the scaffolds between 2 rubber rings at the bottom of a measuring tube filled with 10 cm of water. To keep the water level as even as possible during flow, the tube was kept in contact with a large-diameter reservoir. Before each test, the sample was preconditioned in water for 24 hours. The flow resistance of each scaffold was then evaluated by recording the time required for 10 mL of water to flow through the pores.

4.3.5 Biological Characterization of PCL, PCL/HA and NaOH Treated

PCL/HA Scaffolds

Cell Culture and Cell Seeding

Mouse fibroblasts (L929) and mouse calvaria-derived pre-osteoblastic cells (MC3T3-E1) were used as reference cell lines. L929 cells were cultured as a monolayer in Dulbecco's modified Eagle's medium (DMEM; Sigma-Aldrich, USA) supplemented with 10% fetal bovine serum (FBS; BIOCHROM AG), 1% L-glutamine (Invitrogen Corp., USA), and a 1% antibiotic and antimycotic formulation [containing penicillin G sodium, streptomycin sulfate, and amphotericin B (Invitrogen Corp., USA)]. MC3T3-E1 cells were cultured in Minimum Essential Medium (with Earle's Balanced Salts) (MEM; Hyclone, USA) supplemented with 10% FBS, 1% L-glutamine, and 1% antibiotic and antimycotic formulation. The medium was replaced every 2 days, and the cultures were maintained at 37 °C in a humidified atmosphere with 5% CO₂.

Each scaffold was cut into circular discs (approximately 15 mm in diameter), and the disc specimens were placed in separate wells of a 24-well tissue-culture polystyrene plate (TCPS; Biokom Systems, Poland). The discs were later sterilized in 70% ethanol for 30 min, washed with autoclaved de-ionized water and PBS, and subsequently immersed in MEM overnight. To ensure complete contact between the specimens and the wells, the specimens were pressed with a metal ring (approximately 12 mm in diameter). MC3T3-E1 cells were trypsinized [0.25% trypsin containing 1 mM EDTA (Invitrogen Corp., USA)] and counted with a hemacytometer (Hausser Scientific, USA). MC3T3-E1 cells were seeded at a density of approximately 40,000 cells/well for an attachment-and-proliferation study in which cell viability was quantified with an Alamar blue assay. The cells were also seeded at a density of 80,000 cells/well for an attachment-and-proliferation study in which the morphologies of cultured cells, scaffold specimens, and empty control wells were observed. To determine indirect cytotoxicity, alkaline phosphatase activity, and mineralization, MC3T3-E1 cells were seeded at a density of approximately 40,000 cells/well on the scaffold specimens and in empty wells of the TCPS. The culture was maintained in an incubator at 37 °C in a humidified

atmosphere with 5% CO₂.

Indirect Cytotoxicity Evaluation

Two types of cells were used: 1) mouse calvaria-derived pre-osteoblastic cells (MC3T3-E1) and 2) mouse fibroblasts (L929). An indirect cytotoxicity test was conducted on the TCPS, PCL, PCL/HA, and NaOH-treated PCL/HA scaffolds. First, extraction media were prepared by immersing samples (approximately 15 mm in diameter) in a serum-free medium (SFM) for 1, 3, or 7 days. For L929 cells, the SFM contained DMEM, 1% L-glutamine, 1% lactalbumin, and 1% antibiotic and antimycotic formulation. For MC3T3-E1 cells, the SFM contained MEM, 1% L-glutamine, 1% lactalbumin, and 1% antibiotic and antimycotic formulation. Each extraction medium was used to evaluate the cytotoxicity of the scaffolds. L929 and MC3T3-E1 cells were separately cultured in wells of a 24-well culture plate in 10% serum-containing DMEM and MEM, respectively, for 16 h; this incubation period was sufficiently long to allow cell attachment on the plate. Cells were then starved with SFM for 24 h; subsequently, the medium was replaced with an extraction medium. After 24 hours of cell culture in the extraction medium, a 3-(4,5-dimethylthiazol-2-yl)-2,5-diphenyl-tetrazolium bromide (MTT) assay was carried out to determine the number of viable cells. The experiments were carried out in triplicate.

MTT Assay

The MTT assay is based on the reduction of yellow tetrazolium salt to purple formazan crystals by dehydrogenase enzymes secreted from the mitochondria of metabolically active cells. The amount of purple formazan crystals formed is proportional to the number of viable cells. First, each culture medium was aspirated and replaced with 400 μ L/well of MTT solution at 0.5 mg/mL in a 24-well culture plate. Second, the plate was incubated for 30 minutes at 37 °C. The solution was then aspirated, and 1 mL/well of dimethylsulfoxide (DMSO) containing 125 μ L/well of glycine buffer (pH 10) was added to dissolve the formazan crystals. Finally, after 5 min of rotary agitation, the absorbance of the DMSO solution at 540 nm was measured with a Thermospectronic Genesis10 UV/Visible spectrophotometer.

Cell Attachment and Proliferation

Cell characteristics such as adhesion and proliferation reflect the initial phase of cell–scaffold communication and can affect cell differentiation and mineralization. For the attachment study, MC3T3-E1 cells were allowed to attach to TCPS, PCL, PCL/HA, and NaOH-treated PCL/HA dual-leached scaffolds for 4, 8, or 16 hours. Each sample was rinsed with PBS to remove unattached cells prior to morphological observation. Cell morphology was observed by SEM during the attachment period. For the proliferation study, the viability of cells for each specimen was determined after 1, 2, and 3 days of cell culture with the Alamar Blue assay. The experiments were carried out in triplicate.

Alamar Blue Assay

Resazurin, the active ingredient of the Alamar Blue reagent, is a non-toxic, cell-permeable compound that is blue and virtually non-fluorescent. Once inside cells, resazurin is reduced to resorufin, a red highly fluorescent compound. Viable cells continuously convert resazurin to resorufin, increasing the overall fluorescence and color of the media surrounding the cells. First, each culture medium was removed and replaced with 500 μ L/well of 10% Alamar Blue solution in a 24-well culture plate. Second, the plate was incubated for 3 hours at 37 °C. Finally, the fluorescent emission intensity of the obtained solution was measured at 585 nm with the microplate reader after the sample had been excited at 570 nm.

Morphological Observation of Cultured Cells

After the culture medium was removed, the cell-cultured scaffold specimens were rinsed twice with PBS, and the cells were fixed with 500 μ L/well of a 3% glutaraldehyde solution diluted from a 50% glutaraldehyde solution (Sigma, USA) with PBS. After 30 min, the cells were rinsed again with PBS. After the cells were fixed, the specimens were dehydrated in ethanol solutions of increasing concentration (30%, 50%, 70%, 90%, and 100%) for approximately 2 min at each concentration. The specimens were dried in 100% hexamethyldisilazane (HMDS; Sigma, USA) for 5 min and air-dried after removal of the HMDS. Once completely dry, the specimens were mounted on an SEM stub, coated with gold, and observed with a JEOL JSM-5200 scanning electron microscope (SEM).

Alkaline Phosphatase Activity (ALP)

The alkaline phosphatase (ALP) activity of MC3T3-E1 cells was measured with Alkaline Phosphate Yellow Liquid. In this reaction, ALP catalyzes the hydrolysis of a colorless organic phosphate ester substrate (*p*-nitrophenyl phosphate - pNPP) to yield a yellow product (*p*-nitrophenol) and phosphate. MC3T3-E1 cells were cultured on the scaffold specimens for 3, 5, or 7 days to observe the production of ALP. The specimens were rinsed twice with PBS after the culture medium was removed. Alkaline lysis buffer (10 mM Tris-HCl, 2 mM MgCl₂, 0.1% Triton-X100, pH 10, 200 μL/well) was added, and the samples were scraped and frozen at -20 °C for at least 30 min before proceeding. For each well, 10 μL of 0.1 M amino propanol was mixed with 100 μL of 2 mM MgCl₂; *p*-nitrophenyl phosphate was added at a concentration of 2 mg/ml, and the resulting solution (110 μL) was added to the sample. The specimens were incubated at 37 °C for 15 min. The reaction was stopped with the addition of 900 μL/well of 50 mM NaOH. The extracted solution was transferred to a cuvette and placed in the UV-visible spectrophotometer; the absorbance was measured at 410 nm. The amount of ALP was then calculated against a standard curve. To calculate ALP activity in the cells, the amount of ALP was normalized by the amount of total protein synthesized. For the protein assay, the samples were treated in the same manner as in the ALP assay until the specimens were frozen. After freezing, bicinchoninic acid (BCA; Pierce Biotechnology, USA) solution was added to the specimens. The specimens were incubated at 37 °C for 15 min. The absorbance of the medium was then measured at 562 nm with the UV-visible spectrophotometer, and the amount of the total protein was calculated against a standard curve.

Mineralization Analysis

Alizarin Red-S is a commonly used stain for evaluating calcium deposition. Alizarin Red-S is a dye that binds selectively to calcium salts and is widely used for mineral staining. The isolated osteoblastic cells were plated in 24-well plates at a concentration of 40,000 cells/well and grown in culture medium. After 24 hours, the cultures were treated with culture medium supplemented with 50 μg/mL ascorbic acid (Sigma, USA), 5 mM β-glycerophosphate (Sigma, USA), and

0.2 $\mu\text{g/mL}$ dexamethasone (Sigma, USA). The medium was replaced every 2 days. After 14 and 21 days of treatment, cells were washed with PBS and fixed with ice-cold absolute methanol for 10 min. Fixed cells were stained with 1% Alizarin Red in deionized water (Sigma, USA), pH 4.2, for 2-3 min. After removing alizarin red-S solution, the cells were rinsed with deionized water and dried at room temperature. Images of each culture were captured, and the stain was extracted with 10% cetylpyridinium chloride (Sigma, USA) in 10 mM sodium phosphate for 1 hour. The absorbance of the collected dye was read at 570 nm in a spectrophotometer (Thermo Spectronics Genesis10 UV-visible spectrophotometer).

4.3.6 Statistical analysis

Values are expressed as means \pm standard deviations. Statistical analyses of different data groups were performed by one-way analysis of variance (ANOVA) with the least-significant difference (LSD) test using SPSS software version 11.5. Values of p lower than 0.05 were considered statistically significant.

4.4 Results and Discussion

4.4.1 Characterization of HA

The TEM images of HA nanoparticles dispersed in ethanol are shown in Figure 4.1. The HA nanoparticles were acicular crystals and were on average 140 nm long and 20 nm wide. The XRD pattern of the HA particles is shown in Figure 4.2. The HA nanoparticles exhibited several sharp peaks at the 2θ regions of 26° , 32° , 33° , and 53° , which correspond to the (002), (300), (211), and (004) refraction planes; these peaks are consistent with the crystalline nature of HA nanoparticles. The XRD pattern of the synthesized HA corresponded to an HA phase (JCPDS card no. 9-432). For HA powders, the crystallite size in a direction perpendicular to the crystallographic plane was estimated with Scherrer's equation:

$$d = \frac{(0.9\lambda)}{FWHM \cdot \cos \theta}$$

Here, d is the crystallite size (nm), and $\lambda = 0.15406$ nm for Cu $K\alpha$ radiation of the X-ray beam. FWHM is the full width at half maximum for the diffraction peak (rad), and θ is the Bragg angle of the (002) diffraction angle ($^\circ$). The

crystallite size of HA, which was determined from the inverse of the half value breadth of the (002) peak of HA with Scherrer's equation, had a value of 27.60 nm, as shown in Table 4.1.

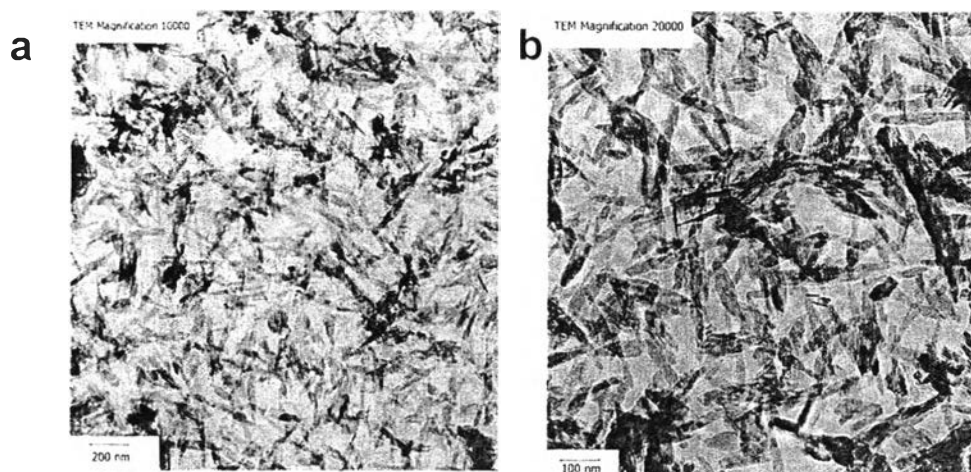
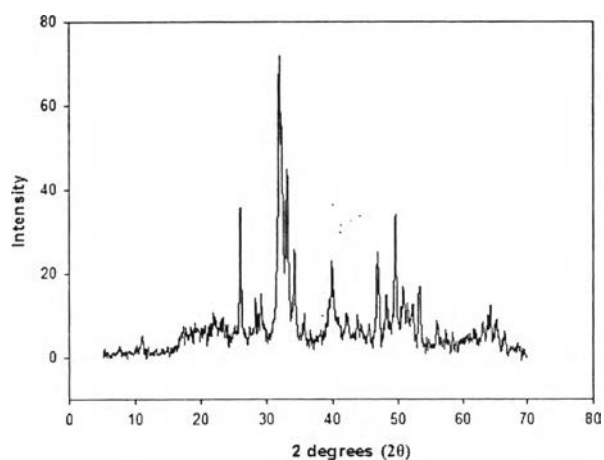
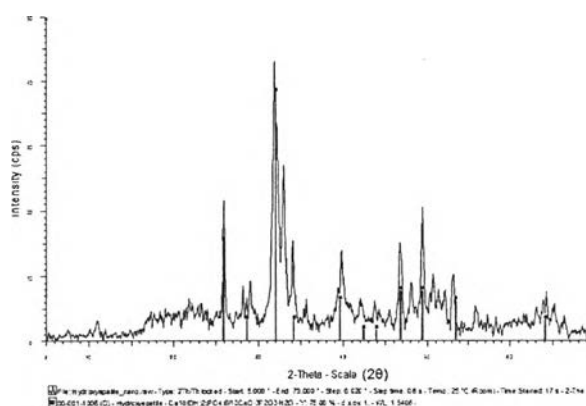


Figure 4.1 TEM images of hydroxyapatite powder at (a)10000x magnification (b)20000x magnification.



(a)



(b)

Figure 4.2 (a) XRD pattern of hydroxyapatite powder (b) Diffraction pattern of HA corresponding to JCPDS card no. 9-432.

Table 4.1 Crystallite size of hydroxyapatite powder

Crystal plane (002)	$2\theta(^{\circ})$	FWHM	Crystallite size (nm)
HA	25.941	0.313	27.60

4.4.2 Characterization of PCL, PCL/HA and NaOH treated PCL/HA scaffolds

Microstructure Observation

Table 4.2 shows the SEM micrographs of the microporous scaffolds formed by PCL-PEG and PCL-PEG/HA blends after leaching in aqueous medium. Well-defined and interconnected pores were produced when both salt and PEG were used, as detected by SEM analysis of the PCL dual-leached scaffold. The interconnected pores were formed in the scaffolds after PEG was leached out. SEM images of PCL/HA and NaOH-treated PCL/HA dual-leached scaffolds showed that both scaffold types had a similar porous structure. In contrast, the PCL dual-leached scaffold had a different porous structure. The pore dimensions of the PCL, PCL/HA, and NaOH-treated PCL/HA dual-leached scaffolds were in the range of $452\pm 31\ \mu\text{m}$, $441\pm 23\ \mu\text{m}$, and $450\pm 29\ \mu\text{m}$, respectively (Table 4.3). The pore size of the PCL dual-leached scaffold was larger than that of the PCL/HA or NaOH-treated PCL/HA dual-leached scaffolds, and more interconnected channels were distributed throughout the PCL dual-leached scaffold. SEM images revealed that the PCL/HA and NaOH-treated PCL/HA dual-leached scaffolds had lower microporosities than the PCL dual-leached scaffold, indicating that HA particles affected the processing of the scaffold. Moreover, the images showed that the macropore interconnectivity and the presence of HA particle aggregates distributed within and on the PCL matrix were maintained.

Table 4.2 SEM images at 50x, 200x, and 750x magnification illustrating the microstructures of the PCL, PCL/HA, NaOH treated PCL/HA dual-leached scaffolds

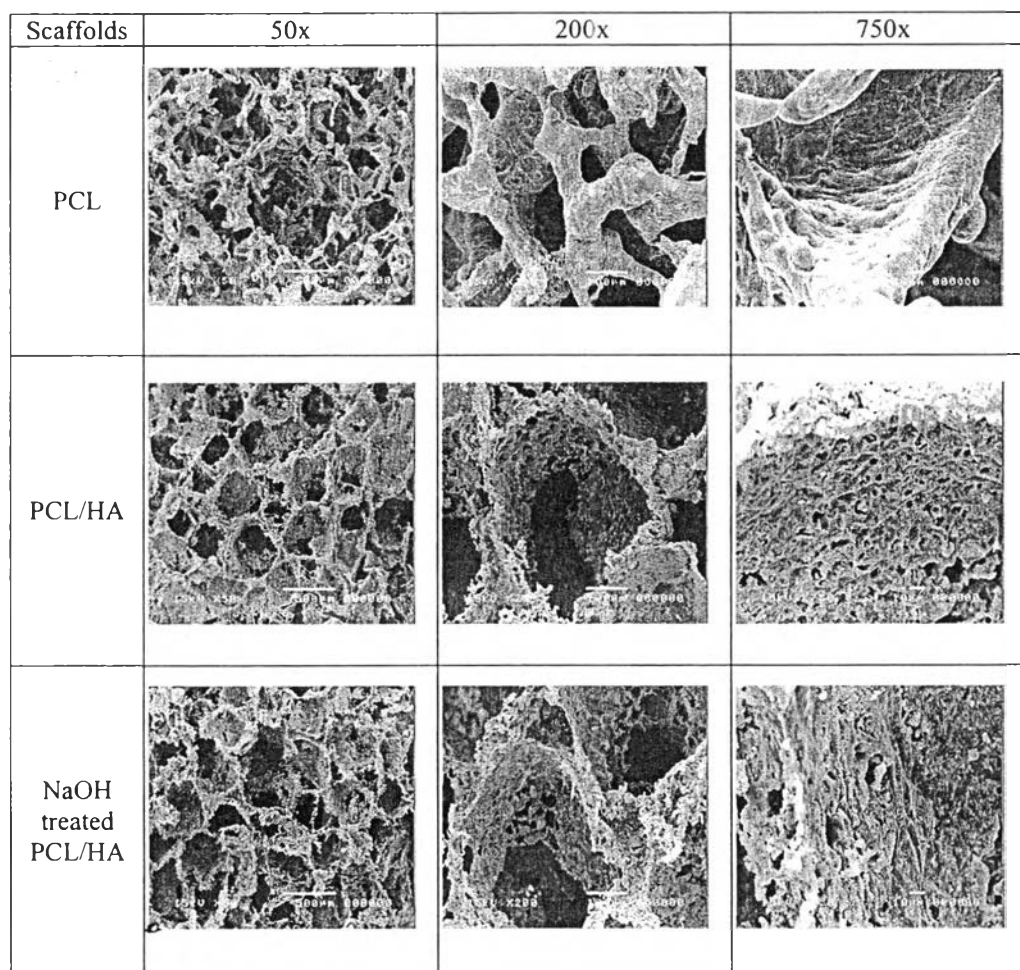


Table 4.3 Pore size of the PCL and PCL/HA dual-leached scaffolds: a,b,c are significantly different at $p < 0.05$ for an individual feature; *one way ANOVA with Tukey HSD, and $n = 30$ for pore size

Scaffolds	Pore Size (μm)
PCL	452 \pm 31
PCL/50% HA	441 \pm 23
NaOH treated PCL/50% HA	450 \pm 29

Actual Amount of HA, Density, Porosity, and Pore Volume

The actual amount of HA and the density, porosity, and pore volume of the prepared PCL/HA scaffolds are shown in Table 4.4 as functions of the initial HA content (0-50% w/w). Based on the TGA information on the char contents at 900 °C in the thermograms, the actual amounts of HA particles within the PCL/HA dual-leached scaffolds could be determined. For the PCL/HA dual-leached scaffolds that had been prepared with initial HA contents of 10%, 20%, 30%, 40%, and 50% w/w, the actual amounts of HA were determined to be 5.2%, 8.8%, 15.98%, 22.95%, and 29.28% w/w, respectively. As the initial HA content increased, the difference between the initial and actual content decreased.

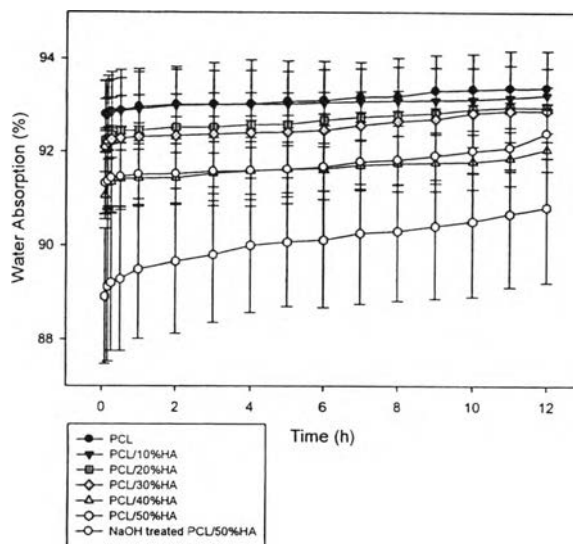
The porosity values of the PCL/HA dual-leached scaffolds were in the range of 71-93% (n=10). The density increased with increasing initial HA content: from approximately 0.085 g/cm³ for the PCL dual-leached scaffold to approximately 0.328 g/cm³ for the scaffold prepared with an initial HA content of 50% (n=10). The porosity decreased from 92.6% for the PCL scaffold to 72.6% for the PCL/50%HA scaffold, and the pore volume decreased from 10.9 cm³g⁻¹ for the PCL scaffold to 2.3 cm³g⁻¹ for the PCL/50%HA scaffold. The pore volume increased with increasing porosity. The presence of HA increased the density but decreased the porosity of the scaffolds. The porosity values decreased in the presence of HA, as HA particles can occupy the free space available in pores.

Table 4.4 Density, percentage of porosity, pore volume, and compressive modulus of the PCL and PCL/HA dual-leached scaffolds: a,b,c,d,e, f are significantly different at $p < 0.05$ for an individual feature; *one way ANOVA with Tukey HSD, and $n = 10$ for porosity pore volume. $n = 30$ for pore size

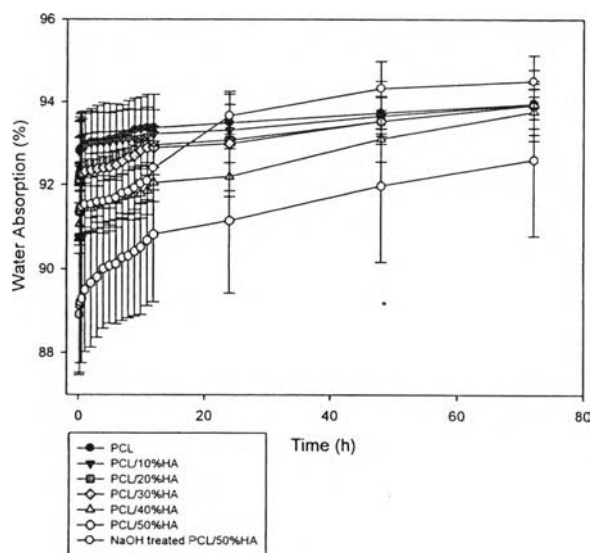
Scaffolds	Actual HA(%)	Density* (g/cm ³)	Porosity* (%)	Pore volume* (cm ³ /g)	Compressive modulus
PCL/No HA	-	0.0853±0.0063 ^{c,d} .e,f	92.55±0.55 ^{c,d,e,f}	10.9104±0.8774 ^{b,c,d} .e,f	57.72±8.24
PCL/10 % HA	5.2214	0.1107±0.0153 ^{d,e} .f	90.33±1.34 ^{d,e,f}	8.3309±1.3976 ^{a,c,d,e,f}	73.84±2.32
PCL/20 % HA	8.824	0.1380±0.0258 ^{a,c} .f	87.95±2.41 ^{a,e,f}	6.6334±1.475 ^{a,b,e,f}	105.93±0.61
PCL/30 % HA	15.9817	0.1552±0.0292 ^{a,b} .e,f	86.44±2.55 ^{a,b,e,f}	5.7621±1.1570 ^{a,b,c,e,f}	148.94±21.46
PCL/40 % HA	22.954	0.3135±0.0286 ^{a,b} .c,d	72.62±2.50 ^{a,b,c,d}	2.3427±0.3224 ^{a,b,c,d}	197.20±9.64
PCL/50 % HA	29.2891	0.3276±0.0396 ^{a,b} .c,d	71.39±3.46 ^{a,b,c,d}	2.2202±0.3820 ^{a,b,c,d}	257.60±24.10

Water Absorption Capacity

Figure 4.3 illustrates the water absorption capacities of the PCL, PCL/HA, and NaOH-treated PCL/HA scaffolds in 0.1 M PBS at room temperature over the course of 3 days. The PCL and PCL/HA scaffolds had similar water absorption capacities. The water absorption rate increased rapidly in the first hour and slightly increased over the course of 3 days. The rate of the PCL/50%HA scaffold increased rapidly in the first 12 hours and continued to increase until the 3 day timepoint. The rate of the NaOH-treated PCL/50%HA scaffold increased rapidly in the first hour and continued to increase for 3 days. The water absorption capacities of the PCL/HA scaffolds were lower than the water absorption capacities of the PCL scaffolds at all time points. With increasing percentages of HA, the water absorption capacities of the scaffolds decreased. The water absorption capacity of the NaOH-treated PCL/50%HA scaffold was higher than that of the PCL/50%HA scaffold and significantly higher than that of the PCL/40%HA scaffold at 12 hours. Moreover, the NaOH-treated PCL/50%HA scaffold had a higher water retention capacity than the other scaffolds. These data confirm that alkaline treatments improve the hydrophilicity of the scaffolds.



(a)



(b)

Figure 4.3 (a) Water absorption capacity of PCL and PCL/HA dual-leached scaffolds in 0.1 M PBS at room temperature over 12 h. (b) Water absorption capacity of PCL and PCL/HA dual-leached scaffolds in 0.1 M PBS at room temperature over 3 days.

Compressive Modulus

The mechanical properties of porous scaffolds are generally evaluated with compressive tests. The compressive moduli of the PCL and PCL/HA scaffolds are shown in Table 4.4. The PCL/HA scaffolds had a higher compressive modulus than the PCL scaffolds. The compressive modulus increased from 58 kPa for the PCL scaffold to 74, 106, 149, 197, and 258 kPa for the PCL/10%HA, PCL/20%HA, PCL/30%HA, PCL/40%HA, and PCL/50%HA scaffolds, respectively. Increasing percentages of added HA resulted in increasing compressive properties of the PCL scaffolds. This finding may have been due to a strengthening effect caused by increasing additions of HA, resulting in a reduced porosity of the scaffold. Cai et al.⁴¹ reported that the tensile, compressive, and shear moduli of crosslinked poly(ϵ -caprolactone) diacrylate(PCLDA)/HA nanocomposites were greatly enhanced by incorporating HA nanoparticles into the polymer matrices. Johari et al.¹¹ also reported that the compressive strength of poly(ϵ -caprolactone)/nano-fluoridated hydroxyapatite(PCL/FHA) scaffolds increased when the weight ratio of FHA was increased.

Table 4.4 Density, percentage of porosity, pore volume, and compressive modulus of the PCL and PCL/HA dual-leached scaffolds: a,b,c,d,e,f are significantly different at $p < 0.05$ for an individual feature; *one way ANOVA with Tukey HSD, and $n = 10$ for porosity pore volume. $n = 30$ for pore size

Scaffolds	Actual HA(%)	Density* (g/cm ³)	Porosity* (%)	Pore volume* (cm ³ /g)	Compressive modulus
PCL/No HA	-	0.0853±0.0063 ^{c,d} .e,f	92.55±0.55 ^{c,d,e,f}	10.9104±0.8774 ^{b,c,d} .e,f	57.72±8.24
PCL/10 % HA	5.2214	0.1107±0.0153 ^{d,e} .f	90.33±1.34 ^{d,e,f}	8.3309±1.3976 ^{a,c,d,e,f}	73.84±2.32
PCL/20 % HA	8.824	0.1380±0.0258 ^{a,c} .f	87.95±2.41 ^{a,c,f}	6.6334±1.475 ^{a,b,e,f}	105.93±0.61
PCL/30 % HA	15.9817	0.1552±0.0292 ^{a,b} .e,f	86.44±2.55 ^{a,b,e,f}	5.7621±1.1570 ^{a,b,e,f}	148.94±21.46
PCL/40 % HA	22.954	0.3135±0.0286 ^{a,b} .c,d	72.62±2.50 ^{a,b,c,d}	2.3427±0.3224 ^{a,b,c,d}	197.20±9.64
PCL/50 % HA	29.2891	0.3276±0.0396 ^{a,b} .c,d	71.39±3.46 ^{a,b,c,d}	2.2202±0.3820 ^{a,b,c,d}	257.60±24.10

Flow Resistance

Figure 4.4 depicts the flow resistance of the PCL, PCL/HA, and NaOH-treated PCL/HA dual-leached scaffolds. The flow resistance ranged from 9.90 to 13.03 sec/10 mL (for a distance of 15-50 cm) for the PCL dual-leached scaffold, from 12.47 to 16.57 sec/10 mL (for a distance of 15-50 cm) for the PCL/HA dual-leached scaffold, and from 13.73 to 18.27 sec/10 mL (for a distance of 15-50 cm) for the NaOH-treated PCL/HA dual-leached scaffold.

For all of the measured distances, the flow resistance was significantly lower for the PCL dual-leached scaffolds than for the PCL/HA and NaOH-treated PCL/HA dual-leached scaffolds. The lower porosity may account for the increased flow resistance observed for the PCL/HA and NaOH-treated PCL/HA dual-leached scaffolds.

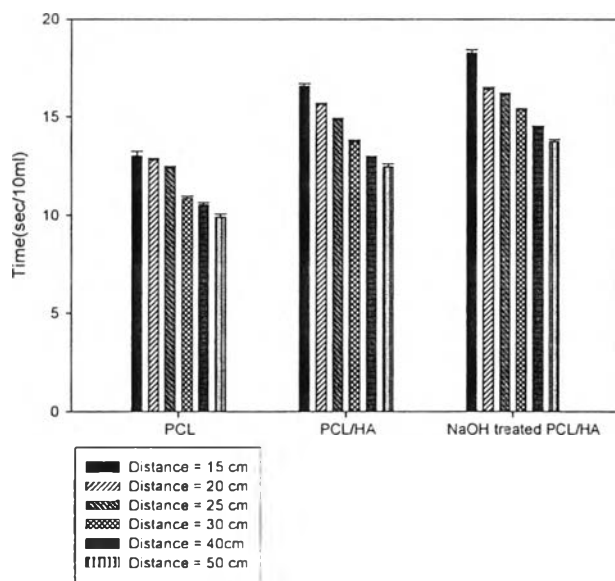
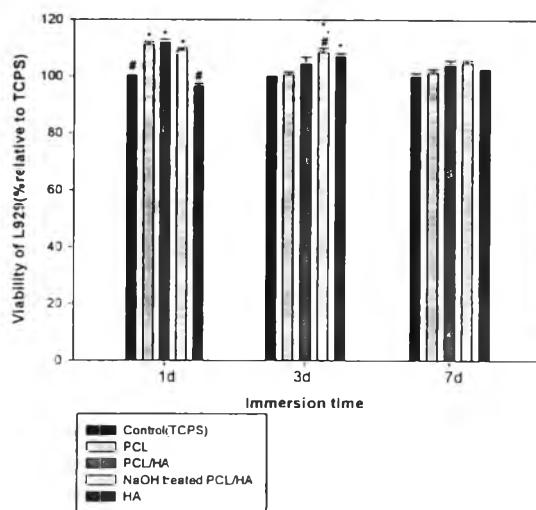


Figure 4.4 Flow resistance of the PCL, PCL/HA, and NaOH treated PCL/HA dual-leached scaffolds.

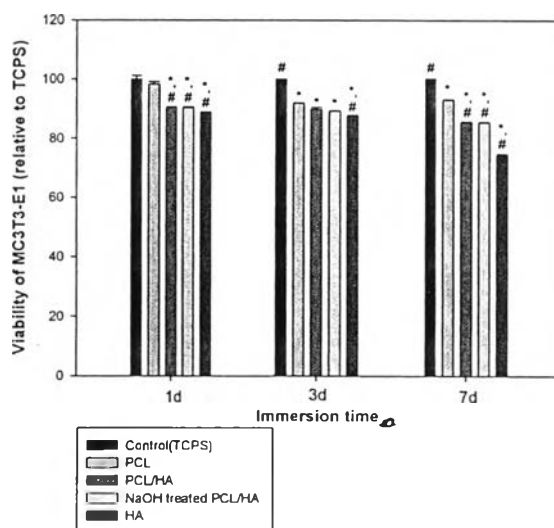
4.4.3 Biological Evaluation of PCL, PCL/HA and NaOH Treated PCL/HA Scaffolds

Indirect Cytotoxicity Evaluation

Indirect cytotoxicity was tested for HA powder, PCL, PCL/HA, and NaOH-treated PCL/HA dual-leached scaffolds with mouse calvaria-derived preosteoblastic cells (MC3T3-E1) and mouse fibroblasts cells (L929). Although we were interested in using the prepared scaffolds as potential bone scaffolds, it was necessary to test the materials with L929 cells to comply with the ISO10993-5 standard test method. For both types of cells, approximately 40,000 cells/well were seeded in empty wells of a TCPS. Figure 4.5 a) and 4.5 b) show the viability of the cells obtained from the MTT assay after the cells had been cultured with the 1-, 3-, or 7-day extraction media. The viability of the cells from the MTT assay was compared to the viability of cells cultured with fresh SFM (control TCPS). The viability of the cells was reported as a percentage of the control value. The viability ratio of cells cultured with extraction media from the PCL dual-leached scaffolds (and with control TCPS) was greater than 80%. This finding suggests that none of the PCL dual-leached scaffolds is cytotoxic.



(a)



(b)

Figure 4.5 Indirect cytotoxic evaluation of TCPS, the PCL, the PCL/HA, the NaOH treated PCL/HA dual-leached scaffolds and HA based on viability of (a) mouse fibroblasts (L929) and (b) pre-osteoblast (MC3T3-E1) that had been cultured with the extraction media from each of these materials against the viability of the cells that had been cultured with the respective culture media for each day as a function of the incubation time of the extraction and the culture media of 1, 3, or 7 d. Statistical significance: * $p < 0.05$ compared with control and # $p < 0.05$ compared to the PCL scaffolds at any given time point.

Cell attachment and cell proliferation

MC3T3-E1 cells were used to test the ability of PCL/HA dual-leached scaffolds to support both the attachment and the proliferation of bone cells. The cells were either seeded or cultured on the surfaces of the PCL dual-leached scaffolds or TCPS (control) for 4, 8 or 16 hours or for 1, 2, or 3 days. Figure 4.6 shows the attachment of MC3T3-E1 cells on the surface of the TCPS and PCL dual-leached scaffolds after 4, 8, and 16 hours of cell culture. The attachment is expressed in terms of the viability of cells (% viability relative to TCPS at 4 hours). The viability of cells on the scaffolds was quantified by fluorescent emission intensity from the Alamar Blue assay. On TCPS, the number of cells increased from 100% at 4 hours of cell culture to 133% at 16 hours of cell culture from an initial seeding density of 40,000 cells/well. The viability of cells on PCL and NaOH-treated PCL/HA dual-leached scaffolds was significantly higher than the viability of cells plated on TCPS; the viability of cells on PCL/HA dual-leached scaffolds was slightly lower at all time points. The viability of cells on NaOH-treated PCL/HA dual-leached scaffold was slightly lower than that of cells on PCL after 4 and 8 hours; however, the viability of cells on the NaOH-treated PCL/HA dual-leached scaffold was slightly higher than that of cells on PCL at 16 hours. The number of cells in the attachment period on the PCL/HA dual-leached scaffold was lower than the number of cells on the NaOH-treated PCL/HA dual-leached scaffolds, possibly due to the lower number of cells that were able to attach to the rough and hydrophobic surface of the PCL/HA dual-leached scaffolds. In contrast, the NaOH-treated PCL/HA dual-leached scaffolds have smoother more hydrophilic surfaces.

Figure 4.7 shows the proliferation of MC3T3-E1 cells on the surface of TCPS and the PCL dual-leached scaffolds on days 1, 2, and 3. Proliferation is expressed in terms of the viability of cells (% relative to TCPS at day 1). The viability of cells on each scaffold was quantified by fluorescent emission intensity from the Alamar Blue assay. On TCPS, the number of cells increased from 100% on day 1 of cell culture to 147% on day 3 from an initial seeding density of 40,000 cells/well. The viability of cells on all PCL dual-leached scaffolds was significantly higher than the viability of cells on TCPS at all time points. On day 1, the viability of cells on the PCL/HA and NaOH-treated PCL/HA dual-leached scaffolds was

significantly lower than the viability of the cells on the PCL dual-leached scaffold; in contrast, the viability of cells on the PCL/HA and NaOH-treated PCL/HA dual-leached scaffolds was greater than the viability of the cells on of the PCL dual-leached scaffold on days 2 and 3. All PCL dual-leached scaffolds were able to support the proliferation of cells at significantly higher levels than TCPS. This finding suggests that the PCL/HA dual-leached scaffolds provided better support for bone cell adhesion and proliferation. The better support of the NaOH-treated PCL/HA dual-leached scaffold for bone cell culture can be attributed to the presence of HA and the improved hydrophilicity of the scaffold promoted by NaOH treatment.

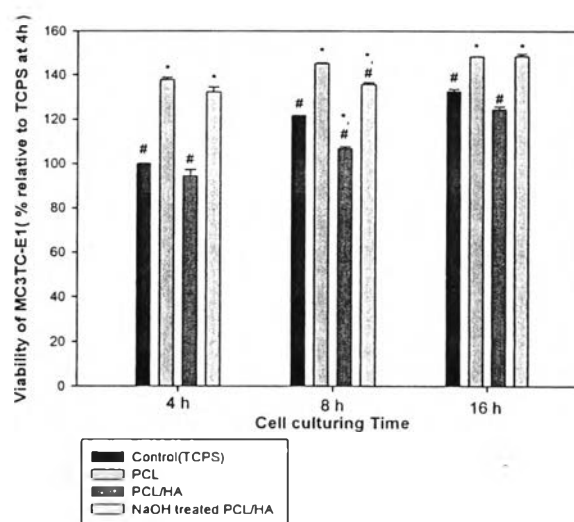


Figure 4.6 Attachment of MC3T3-E1 that had been seeded or cultured on the surfaces of TCPS, the PCL, the PCL/HA and the NaOH treated PCL/HA dual-leached scaffolds for 4, 8, or 16h. Statistical significance: * $p < 0.05$ compared with control and # $p < 0.05$ compared to the PCL scaffolds at any given time.

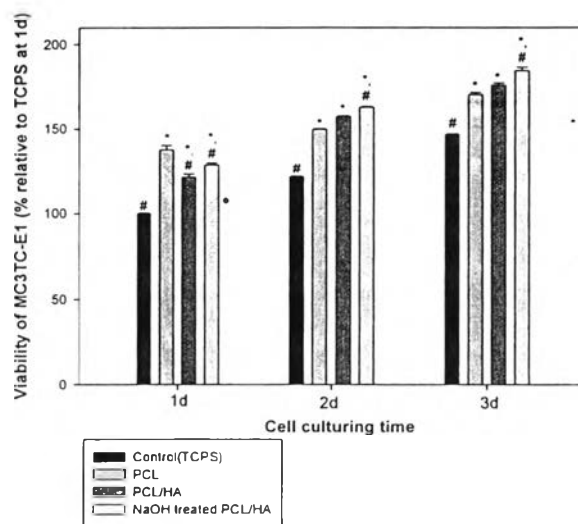


Figure 4.7 Proliferation of MC3T3-E1 that had been seeded or cultured on the surfaces of TCPS, the PCL, the PCL/HA and the NaOH treated PCL/HA dual-leached scaffolds for 1, 2, or 3d. Statistical significance: * $p < 0.05$ compared with control and $^{\#}p < 0.05$ compared to the PCL scaffolds at any given time.

Cell Morphology

Table 4.5 and 4.6 show selected SEM images (magnification = 3500X; scale bar = 5 μm) of MC3T3-E1 cells that were either seeded or cultured on the surfaces of glass, PCL, PCL/HA, and NaOH-treated PCL/HA dual-leached scaffolds at different time points. Using these images, we were able to investigate cell morphology and the interactions between cells. Four hours after cell seeding, the majority of cells on the glass surface displayed a rounded morphology and started to extend their cytoplasm. Eight hours after cell seeding, the majority of cells on the glass surface had extended their cytoplasm on the surface. Within 16 hours of cell seeding, the majority of cells had expanded on the surface. Four hours after seeding, the majority of cells that were seeded on the surface of all scaffolds had expanded on the surface. Eight hours after cell seeding, the majority of cells showed evidence of extension and expansion on the surface. Sixteen hours after cell seeding, the cells on the PCL/HA and NaOH-treated PCL/HA dual-leached scaffolds had expanded the most. At 1, 2, and 3 days after cell seeding, a majority of the cells on the surfaces of

all types of scaffolds had expanded. The greatest expansion was observed on the surface of the NaOH-treated PCL/HA dual-leached scaffold at all time points.

Table 4.5 Attachment of MC3T3-E1 that had been seeded or cultured on the surfaces of glass and the PCL dual-leached scaffolds for 4, 8, or 16 h. Selected SEM images of cultured specimens, i.e., glass (i.e., control), PCL, PCL/HA, and treated NaOH PCL/HA dual-leached scaffolds at three different time points after MC3T3-E1 were seeded or cultured on their surfaces (magnification = 3500X; scale bar = 5 μ m)

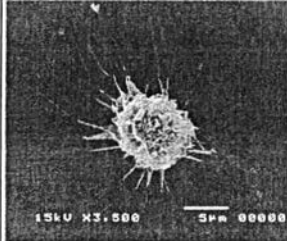

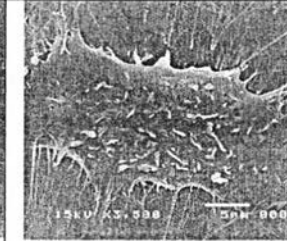
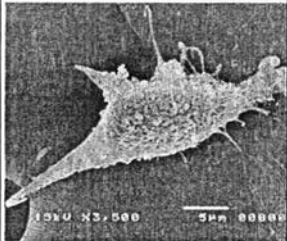
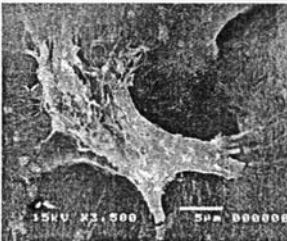
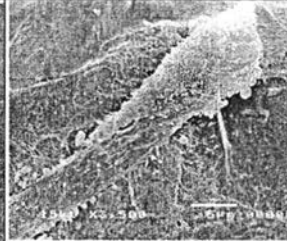



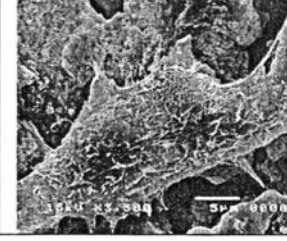


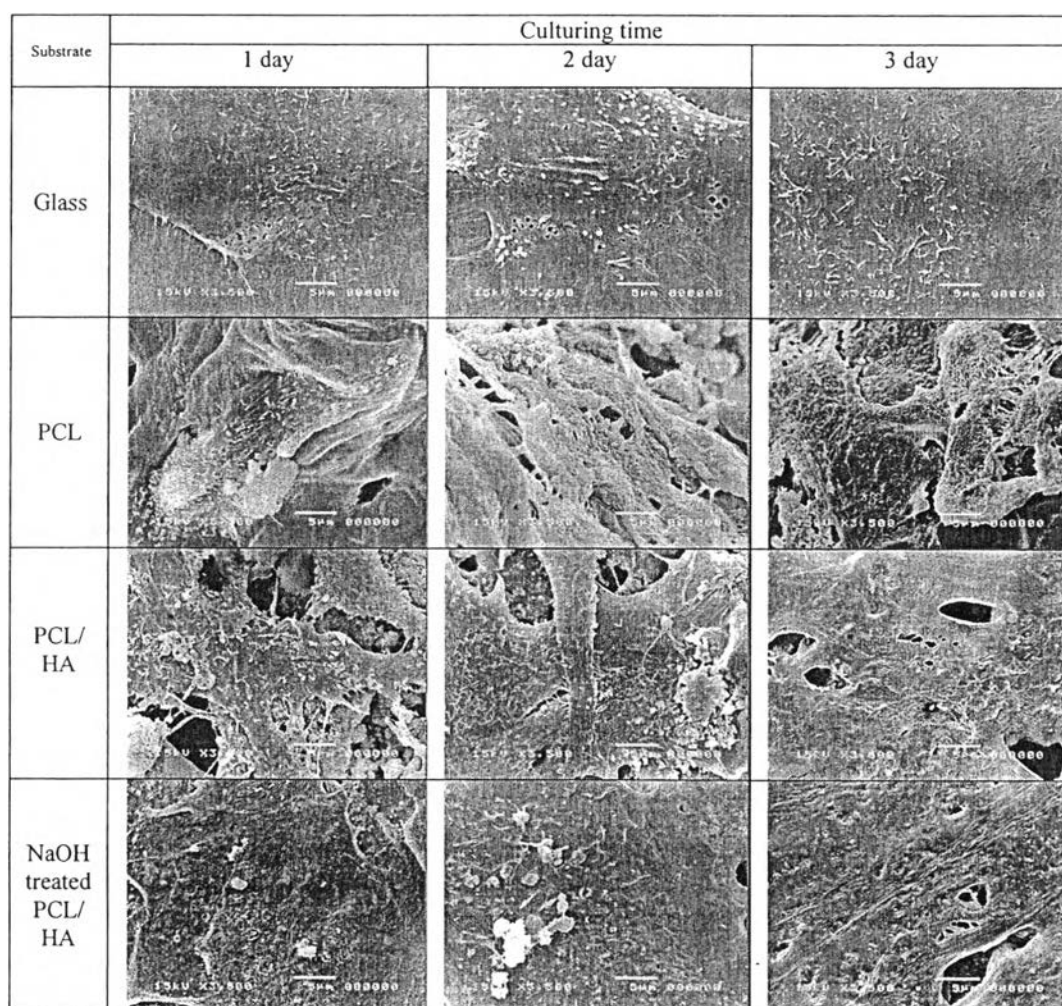
Substrate	Culturing time		
	4 hour	8 hour	16 hour
Glass			
PCL			
PCL/HA			
NaOH treated PCL/HA			

Table 4.6 Proliferation of MC3T3-E1 that had been seeded or cultured on the surfaces of TCPS and the PCL dual-leached scaffolds for 1, 2, or 3d. Selected SEM images of cultured specimens, i.e., glass (i.e., control), PCL, PCL/HA, and NaOH treated PCL/HA dual-leached scaffolds at three different time points after MC3T3-E1 were seeded or cultured on their surfaces (magnification = 3500X; scale bar = 5 μ m)



Alkaline Phosphatase (ALP) Activity

The secretion of alkaline phosphatase (ALP) by osteoblasts is an important indicator of the activity of the cells on a scaffold. The ALP activity of MC3T3-E1 cells cultured on PCL scaffolds for 3, 5, and 7 days was measured. The ALP activity of MC3T3-E1 cells on TCPS (controls), PCL, PCL/HA, and NaOH-treated PCL/HA dual-leached scaffolds was measured at 3, 5, and 7 days of culture

(see Figure 4.8). The ALP activity of cells cultured on PCL scaffolds was lower than that of cells cultured on TCPS at all time points; the only exception occurred with the PCL dual-leached scaffold on day 3. The ALP activity of the cells cultured on PCL/HA and NaOH-treated PCL/HA dual-leached scaffolds was significantly lower than the ALP activity of the cells cultured on the PCL scaffold at all time points. Because ALP activity can also be detected in several non-calcified tissues and organs such as the kidney, small intestines, and placenta, it is possible that the ALP activity of MC3T3-E1 cells that were cultured on scaffolds might not have been a marker of the calcification process.⁴³⁻⁴⁷

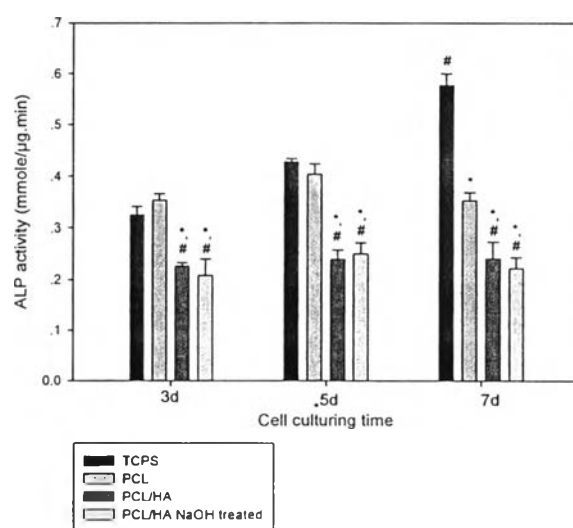


Figure 4.8 Alkaline phosphatase (ALP) activity of MC3T3-E1 that were cultured on the surfaces of TCPS, the PCL, PCL/HA and the NaOH treated PCL/HA dual-leached scaffolds for 3, 5, or 7 d. Statistical significance: * $p < 0.05$ compared with control and # $p < 0.05$ compared to the PCL scaffolds at any given time.

Mineralization

Alizarin Red S staining was used to quantify the mineral deposition of MC3T3-E1 cells that were cultured on the surfaces of TCPS, PCL, PCL/HA, and NaOH-treated PCL/HA dual-leached scaffolds for 14 and 21 days. Table 4.7 shows photographs of the stained specimens. In the presence of calcium, the Alizarin Red S-calcium chelating product appeared red. On day 14 of cell culture, the red staining was greatest for the NaOH-treated PCL/HA dual-leached scaffolds, followed by the PCL/HA, PCL, and TCPS, in that order. An increase in the red staining was observed for all surfaces on day 21. A quantitative analysis of the results shown in Figure 4.9 was carried out by elution of calcium with cetylpyridinium chloride and spectrophotometric measurement at 570 nm. The absorbance measured on day 14 corroborated the aforementioned data; the highest intensity of staining was observed for the NaOH-treated PCL/HA, followed by PCL/HA, PCL, and TCPS, in that order. When the culture was continued until 21 days, a significantly greater amount of calcium deposition was observed for the PCL/HA and NaOH-treated PCL/HA dual-leached scaffolds than for the PCL scaffold and TCPS.

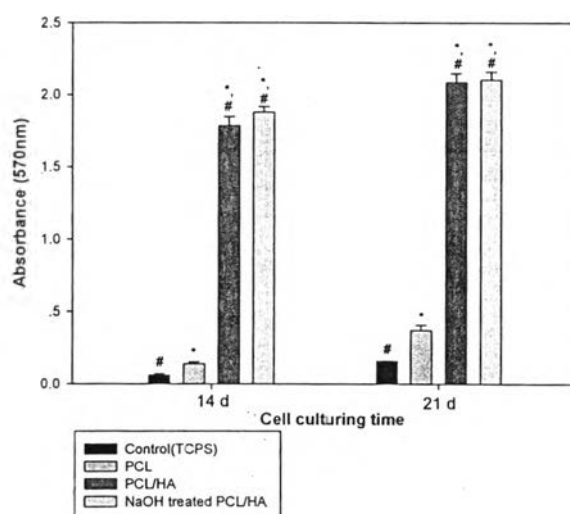
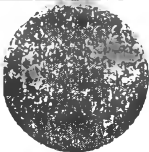
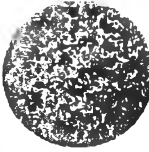
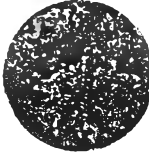
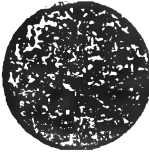

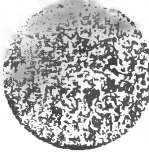

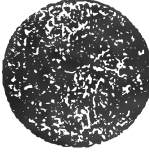



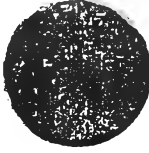



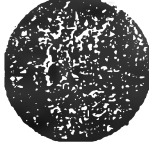


Figure 4.9 Quantification of mineral deposition in MC3T3-E1 by the method of Alizarin Red-S staining. Statistical significance: * $p < 0.05$ compared with control and # $p < 0.05$ compared to the PCL scaffolds at any given time point.

Table 4.7 Images of Alizarin Red-S staining for the mineralization in MC3T3-E1 on the TCPS, the PCL, the PCL/HA and the NaOH treated PCL/HA dual-leached scaffolds at 14 and 21 day

Day		Control(TCPS)	PCL	PCL/HA	NaOH treated PCL/HA
14 Day	+ Cell				
	- Cell				
21 Day	+ Cell				
	- Cell				

4.5 Conclusion

A PCL/HA dual-leached scaffold was prepared by combining solvent casting and salt particulate leaching with a polymer leaching technique. To improve the hydrophilicity of the PCL/HA dual-leached scaffold, the PCL/HA scaffold was treated with an alkaline solution. The PCL, PCL/HA, and NaOH-treated PCL/HA dual-leached scaffolds have been extensively characterized in terms of thermal, physical, and mechanical properties such as morphology, actual HA amount, compressive modulus, and water absorption capacity. The compressive modulus increased from 58 kPa for the PCL scaffold to 258 kPa for the PCL/HA dual-leached scaffolds. The mechanical properties of the PCL/HA dual-leached scaffold were greatly improved by incorporating HA particles as fillers. An indirect evaluation of the cytotoxicity of these scaffolds with mouse fibroblastic cells (L929) and mouse calvaria-derived pre-osteoblastic cell (MC3T3-E1) demonstrated the biocompatibility of these materials for both cell types. The ability of these scaffolds to serve as bone scaffolds was further assessed *in vitro* by measuring the attachment, proliferation, alkaline phosphatase (ALP) activity, and mineralization of MC3T3-E1 cells seeded or cultured at different times. The results showed that the cells cultured on both the PCL and NaOH-treated PCL/HA dual-leached scaffolds exhibited better adhesion than the cells cultured on the TCPS and the NaOH-treated PCL/HA dual-leached scaffolds; similarly, the cells cultured on both the PCL and NaOH-treated PCL/HA dual-leached scaffolds exhibited better proliferation than the TCPS and other scaffolds. Cells that were cultured on dual-leached scaffolds for 4 hours appeared to expand and attach to the scaffold surface, whereas cells that were seeded on the glass substrate retained a round morphology. The cells that were cultured on NaOH-treated PCL/HA dual-leached scaffolds expanded the most on the surface of the scaffold. The assessments of mineralization of MC3T3-E1 cells showed that on days 14 and 21, the staining for calcium deposition of highest intensity was observed for cells grown on the NaOH-treated PCL/HA scaffold, followed by PCL/HA, PCL, and TCPS, in that order. Our results indicate that NaOH-treated PCL/HA dual-leached scaffolds have superior mechanical properties and hydrophilicity; in

addition, their ability to support MC3T3-E1 cell attachment, proliferation, and mineralization makes them potentially useful as bone scaffolding material.

4.6 Acknowledgements

This research work was partially supported by the following funding sources: 1) The Thailand Research Fund (TRF, grant no. DBG5280015 and a doctoral scholarship received from the Royal Golden Jubilee Ph.D. Program, PHD/0100/2551); 2) the "Integrated Innovation Academic Center: IIAC (RES_01_54_63)", Chulalongkorn University Centenary Academic Development Project, Chulalongkorn University; 3) the Petroleum and Petrochemical College (PPC), Chulalongkorn University; 4) the National Center of Excellence for Petroleum, Petrochemicals, and Advanced Materials, Thailand; and 5) the Department of Anatomy, Faculty of Dentistry, Chulalongkorn University.

4.7 References

- [1] Stamatialis DF, Papenburg BJ, Girones M, Saiful S, Bettahalli SNM, Schmitmeier S, Wessling M. Medical applications of membranes: Drug delivery, artificial organs and tissue engineering. *J Membr Sci* 2008; **308**: 1-34
- [2] Tessmar JK, Gopferich AM. Matrices and scaffolds for protein delivery in tissue engineering. *Adv Drug Deliv Rev* 2007; **59**: 274-291
- [3] Carletti E, Motta A, Migliaresi C. Scaffolds for Tissue Engineering and 3D Cell Culture. *Methods Mol Biol* 2011; **695**: 17-39
- [4] Hutmacher DW. Scaffold design and fabrication technologies for engineering tissues--state of the art and future perspectives. *Biomater Sci Polym Ed* 2001; **12** (1): 107-24
- [5] Wang Y, Liu L, Guo S. Characterization of biodegradable and cytocompatible nano-hydroxyapatite/polycaprolactone porous scaffolds in degradation in vitro. *Polym Degrad Stab* 2010; **95**: 207-213
- [6] Bianco A, Federico ED, Moscatelli I, Camaioni A, Armentano I, Campagnolo L, Dottori M, Kenny JM, Siracusa G, Gusmano G. Electrospun poly(ϵ -

caprolactone)/Ca-deficient hydroxyapatite nanohybrids: Microstructure, mechanical properties and cell response by murine embryonic stem cells. *Mater Sci Eng C* 2009; 29: 2063-2071

[7] Roohani-Esfahani SI, Nouri-Khorasani S, Lu Z, Appleyard R, Zreiqat H. The influence hydroxyapatite nanoparticle shape and size on the properties of biphasic calcium phosphate scaffolds coated with hydroxyapatite PCL composites. *Biomater* 2010; 31: 5498-5509

[8] Kim HW, Knowles JC, Kim HE. Hydroxyapatite/poly(ϵ -caprolactone) composite coatings on hydroxyapatite porous bone scaffold for drug delivery. *Biomater* 2004; 25: 1279-1287

[9] Raucci MG, Anto VD, Guarino V, Sardella E, Zeppetelli S, Favia P, Ambrosio L. Biomaterialized porous composite scaffolds prepared by chemical synthesis for bone tissue regeneration. *Acta Biomaterialia* 2010; 6: 4090-4099

[10] Wang Y, Dai J, Zhang Q, Xiao Y, Lang M. Improved mechanical properties of hydroxyapatite/poly(ϵ -caprolactone) scaffolds by surface modification of hydroxyapatite. *Appl Surf Sci* 2010; 256: 6107-6112

[11] Johari N, Fathi MH, Golozar MA. Fabrication, characterization and evaluation of the mechanical properties of poly(ϵ -caprolactone)/nano-fluoridated hydroxyapatite scaffold for bone tissue engineering. *Composites: Part B* 2012; 43: 1671-1675

[12] He L, Zhang Y, Zeng X, Quan D, Liao S, Zeng Y. Fabrication and characterization of poly(L-lactic acid) 3D nanofibrous scaffolds with controlled architecture by liquid-liquid phase separation from a ternary polymer-solvent system. *Polym* 2009; 50: 4128-4138

[13] Wang X, Song G, Lou T. Fabrication and characterization of nano-composite scaffold of PLLA/silane modified hydroxyapatite. *Med Eng Phys* 2010; 32: 391-397

[14] Lee YH, Lee JH, An IG, Kim C, Lee DS, Lee YK, Nam JD. Electrospun dual-porosity structure and biodegradation morphology of Montmorillonite reinforced PLLA nanocomposite scaffolds. *Biomater* 2005; 26: 3165-3172

[15] Woo KM, Seo J, Zhang R, Ma PX. Suppression of apoptosis by enhanced protein adsorption on polymer/hydroxyapatite composite scaffolds. *Biomater* 2007; 28: 2622-2630

- [16] Ngiam M, Liao S, Patil AJ, Cheng Z, Chan CK, Ramakrishna S. The fabrication of nano-hydroxyapatite on PLGA and PLGA/collagen nanofibrous composite scaffolds and their effects in osteoblastic behavior for bone tissue engineering. *Bone* 2009; 45: 4-16
- [17] Dorati R, Colonna C, Genta I, Modena T, Conti B. Effect of porogen on the physico-chemical properties and degradation performance of PLGA scaffolds. *Polym Degrad Stab* 2010; 95: 694-701
- [18] Mao JJ, Xin X, Hussain M. Continuing differentiation of human mesenchymal stem cells and induced chondrogenic and osteogenic lineages in electrospun PLGA nanofiber scaffold. *Biomater* 2007; 28: 316-325
- [19] Shor L, Cuceri S, Wen X, Gandhic M, Suna W. Fabrication of three-dimensional polycaprolactone/hydroxyapatite tissue scaffolds and osteoblast-scaffold interactions in vitro. *Biomater* 2007; 28: 5291-5297
- [20] Liu C, Xia Z, Czernuszka JT. Design and Development of Three-Dimensional Scaffolds for Tissue Engineering. *Chem Eng Res Des* 2007; 85: 1051-1064
- [21] Wei G, Ma PX. Structure and properties of nano-hydroxyapatite/polymer composite scaffolds for bone tissue engineering. *Biomater* 2004; 25: 4749-4757
- [22] Yang F, Cui W, Xiong Z, Liu L, Bei J, Wang S. Poly(L,L-lactide-co-glycolide)/ tricalcium phosphate composite scaffold and its various changes during degradation in vitro. *Polym Degrad Stab* 2006; 91: 3065-3073
- [23] Webster TJ, Ergun C, Doremus RH, Siegel RW, Bizios R. Enhanced functions of osteoblasts on nanophase ceramics. *Biomater* 2000; 21: 1803-1810
- [24] Webster TJ, Siegel RW, Bizios R. Osteoblast adhesion on nanophase ceramics. *Biomater* 1999; 20: 1221-1227
- [25] Webster TJ, Ejiogor JU. Increased osteoblast adhesion on nanophase metals: Ti, Ti6Al4V, and CoCrMo. *Biomater* 2004; 25: 4731-4739
- [26] Ren J, Zhao P, Ren T, Gu S, Pan K. Poly (D,L-lactide)/nano-hydroxyapatite composite scaffolds for bone tissue engineering and biocompatibility evaluation. *J Mater Sci: Mater Med* 2008; 19: 1075-1082

- [27] Kumar PTS, Srinivasan S, Lakshmanan VK, Tamura H, Nair SV, Jayakumar R. β -Chitin hydrogel/nano hydroxyapatite composite scaffolds for tissue engineering applications. *Carbohydr Polym* 2011; 85: 584-591
- [28] Sun F, Zhou H, Lee J. Various preparation methods of highly porous hydroxyapatite/polymer nanoscale biocomposites for bone regeneration. *Acta Biomaterialia* 2011; 7: 3813-3828
- [29] Deplaine H, Gomez Ribelles JL, Gallego FG. Effect of the content of hydroxyapatite nanoparticles on the properties and bioactivity of poly(L-lactide) – Hybrid membranes. *Compos Sci Technol* 2010; 70: 1805-1821
- [30] Ma PX. Biomimetic materials for tissue engineering. *Adv Drug Deliv Rev* 2008; 60: 184-198
- [31] Puppi D, Chiellini F, Piras AM, Chiellini E. Polymeric materials for bone and cartilage repair. *Polym Sci* 2010; 35: 403-440
- [32] Thadavirul N, Pavasant P, Supaphol P. Development of polycaprolactone porous scaffolds by combining solvent casting, particulate leaching, and polymer leaching techniques for bone tissue engineering. *J Biomed Mater Res Part A* 2013; 00A:000-000
- [33] Karageorgiou V, Kaplan D. Porosity of 3D biomaterial scaffolds and osteogenesis. *Biomater* 2005; 26: 5474-5491
- [34] Lee SC, Choi HW, Lee JH, Kim KJ, Chang JH, Kim SY, Choi J, Oh KS, Jeong YK. In-situ synthesis of reactive hydroxyapatite nano-crystals for a novel approach of surface grafting polymerization. *J Mater Chem* 2007; 17: 174-180
- [35] Pena J, Corrales T, Izquierdo-Barba I, Serrano MC, Portolés MT, Pagani R, Vallet-Regí M. Alkaline-treated poly(ϵ -caprolactone) films: Degradation in the presence or absence of fibroblasts. *J Biomed Mater Res* 2006; 76A: 788-797
- [36] Chuenjitkuntaworn B, Inrung W, Damrongsri D, Mekaapiruk K, Supaphol P, Pavasant P. Polycaprolactone/Hydroxyapatite composite scaffolds: Preparation, characterization, and in vitro and in vivo biological responses of human primary bone cells. *J Biomed Mater Res A* 2009; 241-251

- [37] Hariraksapitak P, Suwantong O, Pavasant P, Supaphol P. Effectual drug-releasing porous scaffolds from 1,6-diisocyanatohexane-extended poly(1,4-butylene succinate) for bone tissue regeneration. *Polym* 2008; 49: 2678-2685
- [38] Sombatmankhong K, Sanchavanakit N, Pavasant P, Supaphol P. Bone scaffolds from electrospun fiber mats of poly(3-hydroxybutyrate), poly(3-hydroxybutyrate-co-3-hydroxyvalerate) and their blend. *Polym* 2007; 48: 1419-1427
- [39] Sangsanoh P, Waleetorncheepsawat S, Suwantong O, Wutticharoenmongkol P, Weeranantanapan O, Chuenjitbuntaworn B, Cheepsunthorn P, Pavasant P, Supaphol, P. In Vitro Biocompatibility of Schwann Cells on Surfaces of Biocompatible Polymeric Electrospun Fibrous and Solution-Cast Film Scaffolds. *Biomacromol* 2007; 8: 1587-1594
- [40] Chuenjitbuntaworn B, Supaphol P, Pavasant P, Damrongsri D. Electrospun poly(L-lactic acid)/hydroxyapatite composite fibrous scaffolds for bone tissue engineering. *Polym Int* 2010; 59: 227-235
- [41] Wutticharoenmongkol P, Sanchavanakit N, Pavasant P, Supaphol P. Novel Bone Scaffolds of Electrospun Polycaprolactone Fibers Filled with Nanoparticles. *J Nanosci Nanotechnol* 2006; 6: 514-522
- [42] Wutticharoenmongkol P, Pavasant P, Supaphol P. Osteoblastic Phenotype Expression of MC3T3-E1 Cultured on Electrospun Polycaprolactone Fiber Mats Filled with Hydroxyapatite Nanoparticles. *Biomacromol* 2007; 8: 2602-2610
- [43] Choi JY, Lee BH, Song KB, Park RW, Kim IS, Sohn KY, Jo JS, Ryoo HM. Expression Patterns of Bone-Related Proteins During Osteoblastic Differentiation in MC3T3-E1 Cells. *J Cell Biochem* 1996; 61(4): 609-618.
- [44] Yu HS, Hong SJ, Kim HW. Surface-mineralized polymeric nanofiber for the population and osteogenic stimulation of rat bone-marrow stromal cells. *Mater Chem Phys* 2009; 113: 873-877.
- [45] Tsukamoto Y, Fukutani S, Mori M. Hydroxyapatite-induced alkaline phosphatase activity of human pulp fibroblasts. *J Mater Sci Mater Med* 1992; 3: 180-183.
- [46] Calvert JW, Marra KG, Cook L, Kumta PN, DiMilla PA, Weiss LE. Characterization of osteoblast-like behavior of cultured bone marrow stromal cells on various polymer surfaces. *J Biomed Mater Res* 2000, 52, 279

[47] Cai L, Guinn AS, Wang S. Exposed hydroxyapatite particles on the surface of photo-crosslinked nanocomposites for promoting MC3T3 cell proliferation and differentiation. *Acta Biomaterialia* 2011; 7: 2185-2199